V European Conference on Computational Fluid Dynamics
ECCOMAS CFD 2010
J. C. F. Pereira and A. Sequeira (Eds)
Lisbon, Portugal,14-17 June 2010

MOUNTAIN WAVE DRAG AMPLIFICATION BY RESONANCE IN FLOW WITH A VERTICALLY OSCILLATING SCORER PARAMETER

Miguel A. C. Teixeira*, José L. Argaín† and Pedro M. A. Miranda*

*CGUL, IDL, University of Lisbon,
Edifício C8, Campo Grande, 1749-016 Lisbon, Portugal
e-mails: mateixeira@fc.ul.pt, pmmiranda@fc.ul.pt
†Department of Physics, University of Algarve
Campus de Gambelas, 8005-139 Faro, Portugal
e-mail: jargain@ualg.pt

Key words: Mountain waves, Gravity wave drag, Resonance, Viscous effects

Abstract. *The behaviour of mountain wave drag in stratified flow over a 2D ridge is investigated for atmospheric profiles where the square of the Scorer parameter is the sum of a constant and a relatively small perturbation varying sinusoidally in the vertical. This is carried out using a linear model where friction is approximated as a Rayleigh damping, and simulations of a non-hydrostatic nonlinear numerical model. In the linear model, the solution to the Taylor-Goldstein equation is expanded in powers of a small parameter proportional to the Scorer parameter perturbation. It is found that the drag may be significantly altered by resonance in the vicinity of* $n/l_0 = 2$*, where* n *is the wavenumber of the Scorer parameter oscillation and* l_0 *is the unperturbed value of the Scorer parameter. Depending on the phase of this oscillation, the drag may be considerably amplified, or may decrease relative to its reference value for a constant Scorer parameter* l_0*. The behaviour of the drag is found to be very sensitive to non-hydrostatic effects and to friction (both of which attenuate its deviation from the reference value). In particular, a finite amount of friction (however small) is necessary to produce the drag maxima that were recently detected by previous authors in a similar setup. In the inviscid limit, however, such maxima are suppressed. This suggests that this drag amplification mechanism may be very sensitive to the turbulence closure used in numerical models, or to numerical diffusion effects.*

1 INTRODUCTION

In a recent paper, Wells and Vosper [4] pointed out several mechanisms through which linear theory may fail in predicting the gravity wave drag associated with stably stratified flow over topography. One of these mechanisms, hitherto unexplored apart from a first allusion in an oceanographic context by Phillips [1] and that of Wells and Vosper, involves an atmosphere with a Scorer parameter that oscillates in the vertical. Wells and Vosper [4] showed that, when the vertical wavenumber of the Scorer parameter oscillation is approximately twice the basic (average) Scorer parameter value, the drag may be amplified by a factor of two or more, even when the amplitude of this oscillation is quite small. This is due to a resonant mechanism, which Wells and Vosper classified as intrinsically nonlinear. However, since this resonance occurs due to the interaction between the internal gravity waves associated with the basic Scorer parameter and the superposed Scorer parameter oscillation (which is not part of the wave field), the corresponding mechanism should in fact be essentially linear. This idea will be demonstrated in this study through calculations using a linear model including a crude representation of friction, and simulations of a fully nonlinear numerical model.

2 THEORETICAL MODEL

Consider mountain waves generated in a stably stratified atmosphere flowing perpendicular to a 2D mountain ridge. If this ridge has relatively small amplitude, the flow may be linearised with respect to a reference state. If additionally steady flow is assumed, the equations of motion relevant to this problem are:

$$U\frac{\partial u}{\partial x} + w\frac{dU}{dz} = -\frac{1}{\rho_0}\frac{\partial p}{\partial x} - \lambda u, \tag{1}$$

$$U\frac{\partial w}{\partial x} = -\frac{1}{\rho_0}\frac{\partial p}{\partial z} + b - \lambda w, \tag{2}$$

$$U\frac{\partial b}{\partial x} + N^2 w = 0, \tag{3}$$

$$\frac{\partial u}{\partial x} + \frac{\partial w}{\partial z} = 0. \tag{4}$$

In these equations u and w are, respectively, the streamwise and vertical velocity perturbations, p is the pressure perturbation, b is the buoyancy perturbation, U is the incoming (mean) wind, N is the Brunt-Väisälä frequency of the incoming flow, ρ_0 is a reference density (assumed constant) and λ is a Rayleigh friction coefficient. λ is only included in the momentum equations for simplicity.

If the ridge is isolated, the flow variables may be expressed along the streamwise direction x as 1D Fourier integrals. Then, if (1)-(4) are combined, the Fourier transform of the vertical velocity perturbation $\hat{w}$ may be shown to satisfy the equation:

$$\hat{w}'' + \left(\frac{l^2}{1 - i\frac{\lambda}{Uk}} - k^2\right)\hat{w} = 0, \tag{5}$$

where $i = \sqrt{-1}$, $l^2(z) = N^2/U^2 - U''/U$ is the square of the Scorer parameter, k is the horizontal wavenumber of the waves, and the primes denote differentiation with respect to height, z. Eq. (5) must be solved subject to the boundary conditions that the flow is tangential to the topography at the surface,

$$\hat{w}(z=0) = iU(z=0)k\hat{h}, \tag{6}$$

where $\hat{h}$ is the Fourier transform of the surface elevation, and that the flow decays to zero as $z \to +\infty$ (this transforms into a radiation boundary condition when $\lambda \to 0$).

In the present study, and following Wells and Vosper [4], the Scorer parameter is assumed to take the form:

$$l^2 = l_0^2 \left[1 + \varepsilon \cos(nz + \phi)\right], \tag{7}$$

where l_0 is a constant reference value, ε is a small parameter, n is the wavenumber of a sinusoidal perturbation superposed on the constant Scorer parameter, and ϕ is the corresponding phase.

Solutions to (5) including (7) may be expanded in powers of ε, as follows:

$$\hat{w} = \hat{w}_0 + \varepsilon\hat{w}_1 + \varepsilon^2\hat{w}_2 + \dots . \tag{8}$$

In practice, it will only be necessary to go up to first order in ε to capture the essential physics of the phenomena under consideration. To this order, (5) together with (7) and (8) lead to:

$$\hat{w}_0'' + \left(\frac{l_0^2}{1 - i\frac{\lambda}{Uk}} - k^2\right)\hat{w}_0 = 0, \tag{9}$$

$$\hat{w}_1'' + \left(\frac{l_0^2}{1 - i\frac{\lambda}{Uk}} - k^2\right)\hat{w}_1 = -\hat{w}_0\frac{l_0^2}{1 - i\frac{\lambda}{Uk}}\cos(nz + \phi). \tag{10}$$

The solutions to (9)-(10) which satisfy the boundary conditions are:

$$\hat{w}_0 = iUk\hat{h}\mathrm{e}^{imz}, \tag{11}$$

$$\hat{w}_1 = \frac{1}{2im}\int_0^{+\infty} \hat{w}_0(s)\frac{l_0^2}{1 - i\frac{\lambda}{Uk}}\cos(ns + \phi)\mathrm{e}^{ims}\,ds\left(\mathrm{e}^{imz} - \mathrm{e}^{-imz}\right) + \frac{1}{2im}\int_0^{z} \hat{w}_0(s)\frac{l_0^2}{1 - i\frac{\lambda}{Uk}}\cos(ns + \phi)\left(\mathrm{e}^{-im(z-s)} - \mathrm{e}^{im(z-s)}\right)ds, \tag{12}$$

where

$$m^2 = \frac{l_0^2}{1 - i\frac{\lambda}{Uk}} - k^2, \tag{13}$$

and it has been assumed that U is a constant, so $U(z=0) = U$. It should be noted that m is a complex quantity, i.e. $m = m_R + im_I$, where m_R is the real part and m_I is the

imaginary part, and that $m_I > 0$. This allows the boundary condition at $z \to +\infty$ to be satisfied.

The aim of the present study is to calculate the gravity wave drag, which is given by

$$D = 2\pi i \int_{-\infty}^{+\infty} k\hat{p}^*(z=0)\hat{h}\, dk, \tag{14}$$

where $\hat{p}$ is the Fourier transform of the pressure perturbation and the asterisk denotes complex conjugate. $\hat{p}$ may also be expressed as a power series of ε, as $\hat{p} = \hat{p}_0 + \varepsilon\hat{p}_1 + \varepsilon^2\hat{p}_2 + ...$, and it can be shown that

$$\hat{p}_0(z=0) = i\rho_0 U^2 \hat{h}\left[m_R + \frac{\lambda}{Uk}m_I + i\left(m_I - \frac{\lambda}{Uk}m_R\right)\right], \tag{15}$$

$$\begin{aligned}\hat{p}_1(z=0) = {} & -i\frac{\rho_0 U^2 l_0^2 \hat{h}}{(4m_R^2 - 4m_I^2 - n^2)^2 + 64m_R^2 m_I^2}\left\{8nm_R m_I \sin\phi\right. \\ & -2\left(4m_R^2 + 4m_I^2 - n^2\right)m_R\cos\phi + i\left[\left(4m_R^2 - 4m_I^2 - n^2\right)n\sin\phi\right. \\ & \left.\left.+2\left(4m_R^2 + 4m_I^2 + n^2\right)m_I\cos\phi\right]\right\}.\end{aligned} \tag{16}$$

The drag can equally be expressed as a power series of ε, as $D = D_0 + \varepsilon D_1 + \varepsilon^2 D_2 + \ldots$. The zeroth-order drag, which corresponds to a situation where the Scorer parameter is constant (and equal to l_0), is given by

$$D_0 = 4\pi\rho_0 |U| U l_0 h_0^2 \int_0^{+\infty} k'|\hat{h}'|^2 \left(m'_R + \frac{\lambda a}{Uk'}m'_I\right) dk', \tag{17}$$

where a and h_0 are, respectively, the half-width and the height of the ridge, $k' = ka$, $\hat{h}' = \hat{h}/(h_0 a)$, $m'_R = m_R/l_0$ and $m'_I = m_I/l_0$. The total drag (correct up to first order in ε) is normalized by D_0, and its final expression is found to be:

$$\frac{D}{D_0} = 1 + \varepsilon\frac{D_1}{D_0} = 1 + 2\varepsilon\frac{\int_0^{+\infty} k'|\hat{h}'|^2 m'_R \frac{(4m_R'^2 + 4m_I'^2 - n'^2)\cos\phi - 4n'm'_I\sin\phi}{(4m_R'^2 - 4m_I'^2 - n'^2)^2 + 64m_R'^2 m_I'^2} dk'}{\int_0^{+\infty} k'|\hat{h}'|^2 \left(m'_R + \frac{\lambda a}{Uk'}m'_I\right) dk'}, \tag{18}$$

where $n' = n/l_0$. As given by (18), D/D_0 is a function of n/l_0, $l_0 a$, $\lambda a/U$, ϕ and ε. Values for these parameters similar to those used by Wells and Vosper [4] (apart from $\lambda a/U$) will be adopted next. It is worth noting that the term in the numerator of (18) proportional to $\sin\phi$ is only non-zero if both $m'_R \neq 0$ and $m'_I \neq 0$. For inviscid flow (i.e. $\lambda = 0$) either $m'_R = 0$ or $m'_I = 0$, so this term will vanish. In contrast, the term proportional to $\cos\phi$ is always non-zero when $m'_R \neq 0$. Both m'_R and m'_I are functions of k' (and of $l_0 a$ and $\lambda a/U$).

Since the results depend on the shape of the orography (although not too much, it is hoped), a form for $\hat{h}'$ must be prescribed. Following Wells and Vosper [4], a bell-shaped ridge will be considered, which has the following dimensionless Fourier transform:

$$\hat{h}' = \frac{1}{2}\mathrm{e}^{-k'}. \tag{19}$$

3 RESULTS

The drag is now calculated based on (18) for $\varepsilon = 0.1$, as in Wells and Vosper [4], and for different values of ϕ, as a function of n/l_0.

3.1 Frictional effects

Fig. 1 shows the sensitivity of the normalized drag to the friction coefficient $\lambda a/U$ for $l_0 a = 5$ (cf. Wells and Vosper [4]). Fig. 1a, 1b, 1c and 1d consider, respectively, the cases $\phi = 0$, $\phi = \pi/2$, $\phi = \pi$ and $\phi = 3\pi/2$. It can be seen that the drag is close to one for most values of n/l_0, but near $n/l_0 = 2$ attains a maximum followed by a minimum (Fig. 1a), a single minimum (Fig. 1b), a minimum followed by a maximum (Fig. 1c), or a single maximum (Fig. 1d). The amplitude of these extrema tends to become smaller as $\lambda a/U$ increases, with one exception. For the cases $\phi = \pi/2$ or $\phi = 3\pi/2$ and $\lambda = 0$ (i.e. in inviscid conditions), the minima and maxima that existed when $\lambda \neq 0$ disappear. Since Fig. 1d corresponds to the case shown explicitly by Wells and Vosper [4] (their Fig. 9), the present results might provide an explanation for why their linear model was unable to detect this drag maximum, and they attributed it to intrinsically nonlinear processes. The linear model used by Wells and Vosper [4] is inviscid (see their Eq. (3)), so, by (18) it

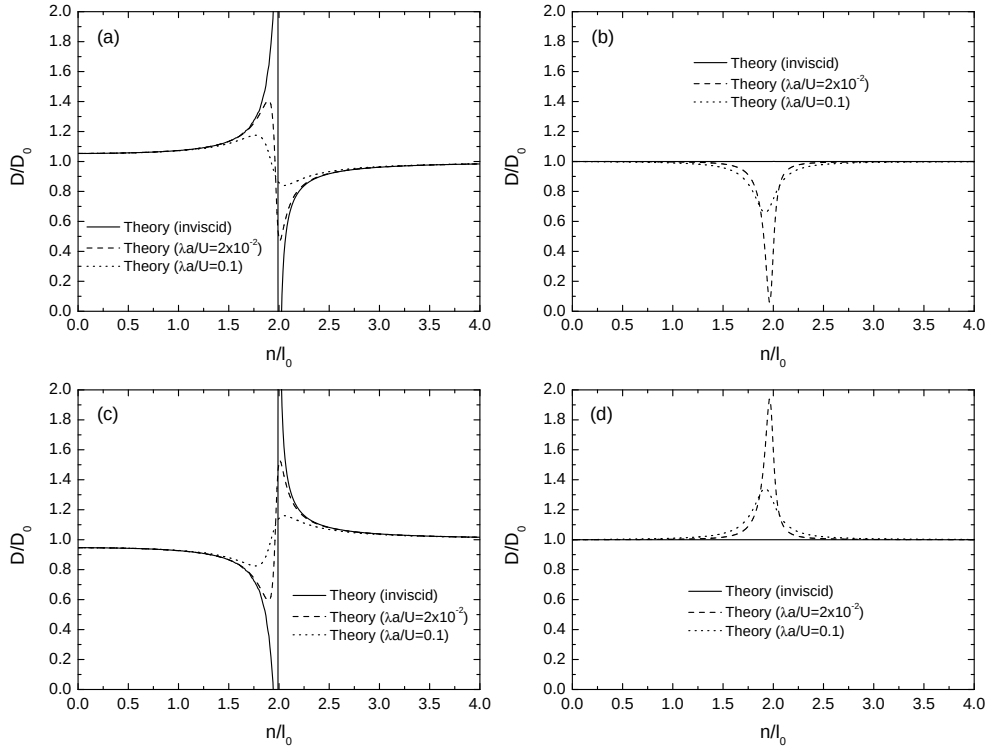

Figure 1: Normalized drag for $\varepsilon = 0.1$, $l_0 a = 5$ and different values of $\lambda a/U$, as a function of n/l_0, for (a) $\phi = 0$, (b) $\phi = \pi/2$, (c) $\phi = \pi$, (d) $\phi = 3\pi/2$.

always gives $D/D_0 = 1$ for $\phi = \pi/2$ or $\phi = 3\pi/2$, because in that situation $\sin\phi = \pm 1$ and $\cos\phi = 0$. This means that only the term proportional to $\sin\phi$ in (18) should contribute to the drag modulation, but that does not happen because in the inviscid case $m'_R m'_I = 0$, making this term zero.

The process responsible for the drag amplification in Fig. 1 is obviously a kind of resonance between the primary mountain wave (generated by a wind profile with constant Scorer parameter l_0) and the oscillation of the Scorer parameter profile, producing harmonics with relatively high energy when $n/l_0 \approx 2$. In the present linear model, this process is symmetric for $\phi = 0$ and $\phi = \pi$ or $\phi = \pi/2$ and $\phi = 3\pi/2$, so Fig. 1c is a mirror image with respect to $D/D_0 = 1$ of Fig. 1a, and the same happens with Fig. 1b and 1d. This is due to the fact that the correction to the drag due to this resonance is treated here as a small perturbation, and implies that the drag could become negative for sufficiently high ε (see next section). Obviously, this unrealistic result only means that the perturbation approach adopted here breaks down in that case.

3.2 Non-hydrostatic effects

Fig. 2 presents essentially similar results to Fig. 1, with the difference that the friction coefficient is kept constant at one of the values employed in Fig. 1 ($\lambda a/U = 2 \times 10^{-2}$)

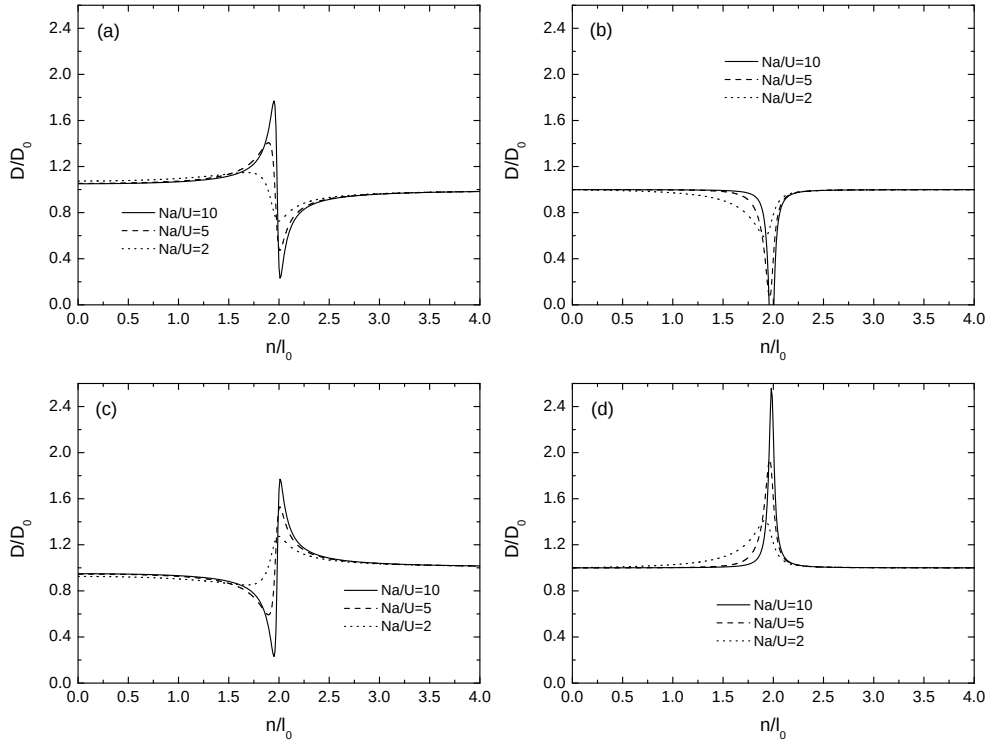

Figure 2: Normalized drag for $\varepsilon = 0.1$, $\lambda a/U = 2 \times 10^{-2}$ and different values of $l_0 a$, as a function of n/l_0, for (a) $\phi = 0$, (b) $\phi = \pi/2$, (c) $\phi = \pi$, (d) $\phi = 3\pi/2$.

and $l_0 a$ is varied. This parameter controls the importance of non-hydrostatic effects: the flow is approximately hydrostatic if it is large, whereas it is strongly non-hydrostatic if it is small. For the three values of $l_0 a$ used, it can be seen that the maxima and minima of the drag corresponding to resonance become smaller as $l_0 a$ decreases. This must be a consequence of wave dispersion moderating the resonant drag amplification. Since resonance relies on trapping by vertical reflections of the energy of the internal gravity waves, dispersion attenuates it by allowing the wave energy to also propagate downstream instead of becoming only concentrated over the mountain. It is curious that non-hydrostatic effects not only attenuate the drag maxima and minima, but they also shift them somewhat to lower values of n/l_0, making these extrema clearly asymmetric.

Since approximately hydrostatic flow increases the amplitude of drag maxima and minima, it can also make the minima lower than zero (as an increase of ε does). This is illustrated, for example, in Fig. 3b for $l_0 a = 10$, and is obviously unrealistic.

3.3 Comparison with numerical results

Fig. 3 shows comparisons of the drag calculated for $\lambda a/U = 2 \times 10^{-2}$ and $l_0 a = 5$ with results from the non-hydrostatic nonlinear numerical model FLEX (see Teixeira et al. [2], [3] for more details) for the same $l_0 a$. The numerical model was run in inviscid mode,

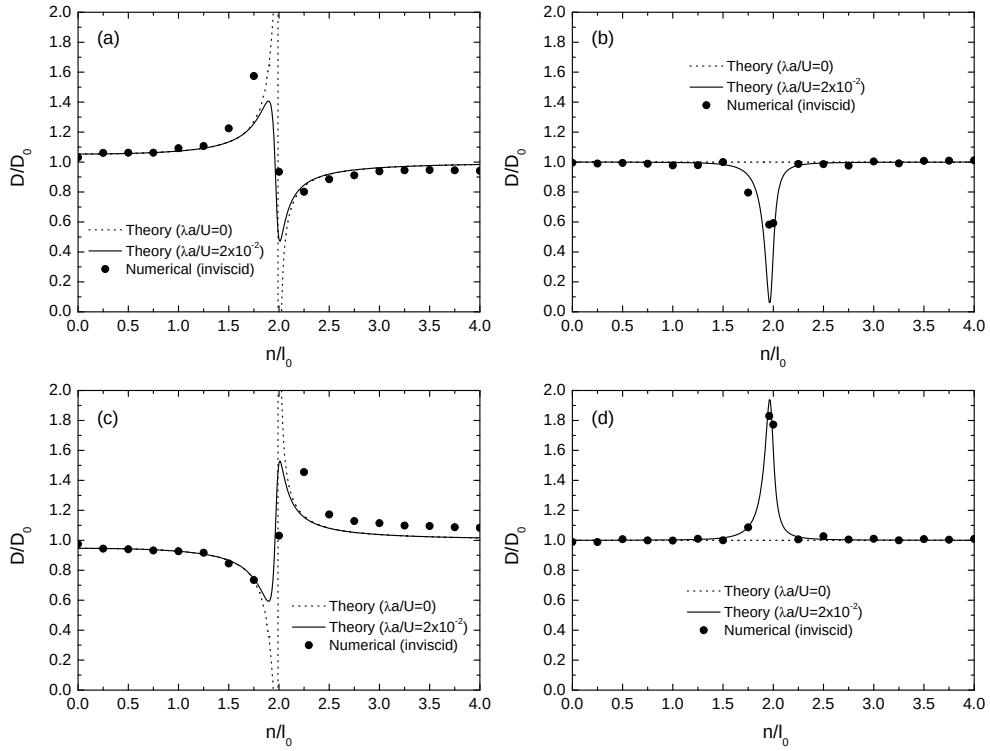

Figure 3: Normalized drag for $\varepsilon = 0.1$ and $l_0 a = 5$, as a function of n/l_0. Lines: analytical model, symbols: numerical model. (a) $\phi = 0$, (b) $\phi = \pi/2$, (c) $\phi = \pi$, (d) $\phi = 3\pi/2$.

as in the crosses of Fig. 9 of Wells and Vosper [4]. It can be seen that, qualitatively, there is agreement between (18) and the numerical model. $\lambda a/U$ has been adjusted to optimally fit the numerical data in Fig. 3d. This leads the drag minimum in Fig. 3b to be underestimated. The reason why the drag maximum is larger than the drag minimum in the numerical simulations is easy to understand: the total drag can never be lower than zero, hence its minima must have limited amplitude. This aspect is not taken into account in the analytical model, as was noted above. There is also some underestimation of the drag maxima in Fig. 3a and 3c, although the drag minima are captured accurately. This must also be related to the assumptions of (18), either that ε must be small, that D is only expanded to first order in ε, or more basic reasons inherent to the linear approximation, for example the very crude representation of friction. Nevertheless, the qualitative behaviour of the numerical data is captured adequately. In Fig. 3 the curve from (18) for $\lambda = 0$ is also shown, to emphasize the crucial role of friction in the cases displayed in Fig. 3b and 3d. As can be seen, even if the numerical simulations are nominally inviscid, they produce a drag behaviour which is attributable to friction. Fig. 9 of Wells and Vosper [4] shows that qualitatively the same behaviour is obtained when a simple turbulence closure is employed. This shows that the frictional process that generates the drag minima or maxima in Fig. 3b or 3d may either be of physical or of numerical origin.

4 CONCLUSIONS

In this study, a mechanism recently re-discovered by Wells and Vosper [4] for the amplification of drag in stratified flow over mountains has been explored in some detail. This mechanism relies on the existence of an environment with a Scorer parameter that oscillates with height, although the amplitude of this oscillation (relative to the basic state) may be relatively modest. The drag is amplified or reduced by a resonant process, leading to relatively large maxima or minima in the vicinity of the parameter space region where $n/l_0 = 2$. This resonant process has a different behaviour depending on the phase of the Scorer parameter oscillation. Either single drag maxima or minima, or adjoining drag maxima and minima may be generated. Both non-hydrostatic effects, due to wave dispersion, or friction, due to energy dissipation, lead to an attenuation of these drag extrema. The situation of a single drag maximum (considered previously by Wells and Vosper [4]), or of a single drag minimum, are found to be very sensitive to friction. Although generally all drag extrema tend to be attenuated as friction increases, single maxima and minima are totally suppressed in purely inviscid flow. This does not happen in numerical simulations, whether they are nominally inviscid or include a turbulence closure. This highlights the crucial role of such closures, or of numerical diffusion, in attaining a physically accurate representation of the mechanism of resonant drag enhancement addressed here.

Numerical simulations including boundary layer effects, using a proper turbulence closure, will be carried out next in order to further understand the effects of friction, and test the simple theoretical model presented in this study.

REFERENCES

[1] O. M. Phillips, The interaction trapping of internal gravity waves. *J. Fluid Mech.*, **34**, 407–416 (1968).

[2] M. A. C. Teixeira, P. M. A. Miranda and J. L. Argaín, Resonant gravity wave drag enhancement in linear stratified flow over mountains, *Quart. J. Roy. Meteorol. Soc.*, **131**, 1795–1814 (2005).

[3] M. A. C. Teixeira, P. M. A. Miranda and J. L. Argaín, Mountain waves in two-layer sheared flows: critical-level effects, wave reflection, and drag enhancement, *J. Atmos. Sci.*, **65**, 1912–1926 (2008).

[4] H. Wells and S. B. Vosper, The accuracy of linear theory for predicting mountain-wave drag: Implications for parametrization schemes, *Quart. J. Roy. Meteorol. Soc.*, **136**, 429–441 (2010).